Fisheries and Oceans Canada | Pêches et Océans Canada
Ecosystems and Oceans Science | Sciences des écosystèmes et des océans

Canadian Science Advisory Secretariat (CSAS)

Research Document 2020/046

Central and Arctic Region

Recovery Potential Modelling of Westslope Cutthroat Trout (*Oncorhynchus clarkii lewisi*) in Designatable Unit 1: Saskatchewan-Nelson River populations

Adam S. van der Lee and Marten A. Koops

Fisheries and Oceans Canada
Great Lakes Laboratory for Fisheries and Aquatic Sciences
867 Lakeshore Rd.
Burlington, ON L7S 1A1 Canada

July 2020

Canada

Foreword

This series documents the scientific basis for the evaluation of aquatic resources and ecosystems in Canada. As such, it addresses the issues of the day in the time frames required and the documents it contains are not intended as definitive statements on the subjects addressed but rather as progress reports on ongoing investigations.

Published by:

Fisheries and Oceans Canada
Canadian Science Advisory Secretariat
200 Kent Street
Ottawa ON K1A 0E6

http://www.dfo-mpo.gc.ca/csas-sccs/
csas-sccs@dfo-mpo.gc.ca

ISSN 1919-5044

Correct citation for this publication:

van der Lee, A.S. and Koops, M.A. 2020. Recovery Potential Modelling of Westslope Cutthroat Trout (*Oncorhynchus clarkii lewisi)* in Canada (Saskatchewan-Nelson River populations). DFO Can. Sci. Advis. Sec. Res. Doc. 2020/046. v + 26 p.

Aussi disponible en français :

van der Lee, A.S., et Koops, M.A. 2020. Modélisation du potentiel de rétablissement de la truite fardée versant de l'ouest (Oncorhynchus clarkii lewisi*) dans l'unité désignable 1 : Populations de la rivière Saskatchewan et du fleuve Nelson. Secr. can. de consult. sci. du MPO, Doc. de rech. 2020/046. v + 29 p.*

TABLE OF CONTENTS

ABSTRACT v
INTRODUCTION 1
METHODS 1
SOURCES 1
LIFE HISTORY 2
Age and Growth 2
Reproduction 2
Mortality 3
THE MODEL 4
Stochasticity 6
Density-dependence 6
IMPACT OF HARM 7
Elasticity of λ 8
Elasticity of N 8
Simulation 8
RECOVERY TARGETS 9
Abundance: Minimum Viable Population (MVP) 9
Habitat: Minimum Area for Population Viability (MAPV) 10
RECOVERY TIMES 11
RESULTS 11
IMPACT OF HARM 11
Elasticity of λ 12
Elasticity of N 13
Simulation 15
RECOVERY TARGETS 16
Abundance: Minimum Viable Population (MVP) 16
Habitat: Minimum Area for Population Viability (MAPV) 18
RECOVERY TIMES 18
DISCUSSION 18
UNCERTAINTIES 21
ELEMENTS 22
Element 1: Estimate the current or recent life-history parameters for WCT 22
Element 2: Propose candidate abundance and distribution target(s) for recovery 22
Element 3: Project expected population trajectories over a scientifically reasonable time frame (minimum 10 years), and trajectories over to the potential recovery target(s), given current WCT population dynamics parameters. 22
Element 4: Provide advice on the degree to which supply of suitable habitat meets the demands of the species both at present and when the species reaches the potential recovery target(s) identified in element 12. 22

Element 5: Assess the probability that the potential recovery target(s) can be achieved under the current rates of population dynamics, and how that probability would vary with different mortality (especially lower) and productivity (especially higher) parameters. 23
Element 6: Evaluate maximum human-induced mortality and habitat destruction that the species can sustain without jeopardizing its survival or recovery. 23
REFERENCES CITED 23

ABSTRACT

The Committee on the Status of Endangered Wildlife in Canada (COSEWIC) assessed the Westslope Cutthroat Trout (WCT, *Oncorhynchus clarkii lewisi*) as Threatened for Saskatchewan-Nelson River populations (DU 1) in Canada. Here population modelling is presented to assess the impacts of harm, determine abundance and habitat recovery targets, and conduct long-term projections of population recovery in support of a recovery potential assessment (RPA). The analysis demonstrated that WCT populations were most sensitive to perturbations to the juvenile stage (e.g. survival, growth, and habitat) under most circumstances. Harm to these aspects of WCT life-history should be avoided. Population viability analysis was used to identify potential recovery targets. Demographic sustainability, (i.e. a self-sustaining population over the long term) can be achieved with population sizes of 1,600 to 4,200 adults (> 138 mm). A population of this size would require between 21 and 37 km of stream habitat. Population projections predicted that recovery could occur in 27–33 years with an initial density of 10% of the abundance targets.

INTRODUCTION

Populations of Westslope Cutthroat Trout (WCT, *Oncorhynchus clarkii lewisi*) within designatable unit (DU) 1, Saskatchewan-Nelson River populations, have been assessed as Threatened by the Committee on the Status of Endangered Wildlife in Canada (COSEWIC). Pacific populations of WCT, DU 2, were assessed as Special Concern by COSEWIC (COSEWIC 2016).

The *Species at Risk Act* (SARA) mandates the development of strategies for the protection and recovery of species that are at risk of extinction or extirpation from Canada. In response, Fisheries and Oceans Canada (DFO) has developed the recovery potential assessment (RPA; DFO 2007a,b) as a means of providing information and scientific advice. There are three components to each RPA - an assessment of species status, the scope for recovery, and scenarios for mitigation and alternatives to activities - that are further broken down into 22 elements. This report contributes to the RPA through use of population modelling to assess the impact of anthropogenic harm to populations, identify recovery targets, and project population recovery with associated uncertainties. This work is based on a demographic approach developed by Vélez-Espino and Koops (2009, 2012) and Vélez-Espino et al. (2010).

This report will focus solely on Saskatchewan-Nelson River populations (DU 1) of WCT. WCT in Alberta have undergone a substantial range contraction and currently occupy < 20% of their historic range (COSEWIC 2016). The continued persistence of populations of WCT is threatened by hybridization with non-native Rainbow Trout (RT, *O. mykiss*) and non-native cutthroat trout, which through stocking, have become widely distributed (COSEWIC 2016). Only genetically pure populations (> 99% WCT alleles) will be considered for protection under SARA. These populations are typically limited to low productivity, cold, high elevation streams where RT are less successful (Rasmussen et al. 2010). Populations in this habitat type typically express the stream resident life-history strategy (Janowicz et al. 2018) which achieve greater longevity and smaller maximum body size than other life-history types.

This report, therefore, presents population modelling of genetically pure, stream resident WCT occupying small, low productivity headwater streams within its native range in Alberta. The results of the analysis apply only to this specific life-history type and will likely not be representative of migratory or lake resident life-history types.

METHODS

Information on vital rates was compiled to build projection matrices that incorporate environmental stochasticity and density-dependence. The impact of anthropogenic harm to populations was quantified with use of elasticity and simulation analyses. Estimates of recovery targets for abundance and habitat were made with estimation of the minimum viable population (MVP) and the minimum area for population viability (MAPV). Finally, simulation analyses were used to project population abundances and make estimates of potential recovery time-frames.

SOURCES

WCT in Alberta is relatively well studied for freshwater species at risk. Janowicz et al. (2018) investigated life-history characteristics of populations of stream resident WCT providing information on: longevity, growth, maturity, survival, and egg production. Much of the parameterization of the model was drawn from this study. While Janowicz et al. (2018) provides important information towards parameterizing the model, it should be noted the data were collected from 2002–2004 when a legal harvest of WCT > 35 cm was permitted and genetic

methods were not able to determine genetic purity at today's standards. As such, four of the six streams sampled by Janowicz et al. (2018) do not meet the 99% requirement for WCT. Additional information was sourced from previous WCT population models such as Hilderbrand (2003) and Paul et al. (2003), as well as studies from other locations such as Montana (Carim et al. 2017). All analyses and simulations were conducted using the statistical program R 3.5.0 (R Core Team 2018).

LIFE HISTORY

Age and Growth

Maximum age, estimated from otoliths, was 13 years for females and 12 years for males for stream resident WCT in Alberta (Janowicz et al. 2018). Historically, WCT were thought to have shorter life-spans, 6-8 years (Behnke 2002); however, other stream resident populations have been documented living beyond age-10 (Fraley and Shepard 2005).

Length-at-age, L_t, of WCT was well described with a von Bertalanffy growth function (VBGF):

$$L_t = L_\infty(1 - e^{-k(t-t_0)}), \quad (1)$$

Where L_t is fork length (FL) in mm at age-t, t_0 is the hypothetical age at which the fish would have had a length of 0, L_∞ is the asymptotic size, and k is a growth parameter. Janowicz et al. (2018) found potential differences in VBGF parameters among locations but no significant difference between sexes. The across location estimates of growth was incorporated into the model where: $L_\infty = 270$, $k = 0.168$, and $t_0 = 0.212$ (Janowicz et al. 2018).

Reproduction

The measured sex ratio in WCT varies among populations (Downs et al. 1997, Janowicz et al. 2018). As a result, an equal number of males and females throughout the life cycle was assumed. Maturity is best determined by length and differs between sexes (Downs et al. 1997). The proportion mature, θ_{FL}, as a function of length for females was described by the relationship (Janowicz et al. 2018):

$$\theta_{FL} = \frac{1}{1+e^{-(0.257FL-35.426)}}, \quad (2)$$

Giving a size-at-50% maturity of 138 mm and age-of-50% maturity of ~ 4.5, consistent with other observations (Downs et al. 1997).

Janowicz et al. (2018) observed only a small increase in egg count with body size where fecundity, f, increased as a linear relationship with fork length:

$$f = 15.15 + 1.19FL\ , \quad (3)$$

This observed slope was significantly less than those estimated in previous studies: 4.4 (Downs et al. 1997), 2.94 (Mayhood 2012), 5.5 (Tripp et al. 1979); however, it may represent the only recent, estimate specific to high elevation, stream resident WCT in Alberta and, therefore, it was incorporated into the population model. There was, however, a significant increase in reproductive investment with body size in the form of increased egg volume with maternal fork length (Janowicz et al. 2018). In addition, Mayhood (2012) provided a relationship between egg diameter (mm) and fork length:

$$E = 0.9553 + 0.0069FL. \quad (4)$$

There is the potential that increased egg size may afford greater early life survivorship in offspring (Duarte and Alcaraz 1989). An assumed relationship between maternal investment

(egg size) and relative egg survival based on maternal size was incorporated into the model. The impact on maternal investment (π) was used to scale egg survival such that the survival of eggs of first maturing females (the smallest size class with mature females, 127 mm) was 65% (Moffett et al. 2006) that of old females (the largest size class of females, 217 mm) such that:

$$\pi_i = 0.564 Egg\ diameter_i - 0.38. \quad (5)$$

Mortality

Numerous estimates of adult instantaneous mortality, *Z*, were available for WCT, however, they varied widely. Many of the sampled populations may have been subject to an unknown level of fishing mortality. The model does not take fishing mortality, *F*, into account and therefore estimates of total instantaneous mortality, *Z*, are treated as natural mortality, *M*, ($Z = M + F$). Carim et al. (2017) used catch-curve analysis to estimate adult mortality for various populations of WCT in Montana with individuals aged with use of location specific length keys giving estimates ranging from 0.82 to 1.37 (survival rates of 25–44%). Janowicz et al. (2018) used catch curve analysis to provide an across population estimate of *Z* for Alberta WCT of 0.55 (survival rate of 58%). Rasmussen et al. (2010) used catch curve analysis to estimate *Z* for an Alberta population of pure WCT and WCT X RT hybrids finding the pure WCT mortality was lower, 0.36 (survival rate of 70%) than hybrids, 0.6 (survival rate of 55%). Finally, Cope et al. (2016) estimated *Z* for telemetry tracked WCT in British Columbia to be between 0.24 and 0.31 (survival rate of 68–79%).

The literature reports of mortality were compared to two predicted values from across-species relationships (Then et al. 2015) where *M* is a function of longevity:

$$M = 4.899 {t_{max}}^{-0.916}, \quad (6)$$

or VBGF parameters:

$$M = 4.118 k^{0.73} {L_\infty}^{-0.33}. \quad (7)$$

The predictive relationships give estimates of mortality of 0.47 (survival rate of 0.63) and 0.18 (survival rate of 0.84) respectively.

No estimates for juvenile survival rate were available for WCT, however, juvenile survival has been estimated for other cutthroat trout (CT) subspecies such as Colorado River Cutthroat Trout (CRCT; *O. c. pleuriticus*) and Bonneville Cutthroat Trout (BCT; *O. c. utah*). Juvenile survival of CT generally increased with age and body size (Peterson et al. 2004, Budy et al. 2007). Peterson et al. (2004) estimated survival rate of juvenile CRCT with Brook Trout (*Salvelinus fontinalis*) absent and present. Survival rates were lower with Brook Trout present with estimates of 2.5%, 23% and 35–57% annual survival for ages 0, 1, and 2+ CRCT compared to 32%, 42% and 37–53% when Brook Trout were absent. Budy et al. (2007) estimated annual survival rates for juvenile BCT, 41% at age-1, 46% at age-2 and 54% at age-3.

Budy et al. (2012) estimated *in situ* egg survival rates for BCT at various locations in Utah. Mean survival rates varied within and among sampling locations ranging from 43% to 77% and averaged 67% at high elevation sites (Budy et al. 2012).

The literature values were used to inform model parameters for stage-specific survival rates. As density-dependence was incorporated into the population model (see below) parameter values for stage-specific survival (σ_i) were required for stable populations (population growth rate (λ) equal to 1) and populations growing at maximum rates ($\lambda = \lambda_{max}$, when density is 0). With $\lambda = 1$, mean adult survival (σ_a) was assumed to be 0.6, an intermediate value from literature estimates and similar to the predicted value from the relationship with longevity (Equation 6). Juvenile survival was assumed to be less than adult survival and increase with size (Lorenzen 2000) with

mean survival rates for stages 1 to 4 set to 0.3, 0.4, 0.5, and 0.55 respectively. Egg survival (σ_e) was assumed to be 0.65. Young-of-Year (YOY) survival (σ_0) was solved for to give λ = 1 which resulted in a value of ~ 0.18.

At maximum population growth rate (λ_{max}) mean adult survival was set higher than the observed values and based around the predicted value from the relationship VBGF (Equation 7) parameters and assumed to be 0.85. Maximum egg survival was assumed to 1. Maximum survival for other stages were assumed to scale the same as the adult stages $\sigma_{i,max} = \sigma_{i,1} \times \sigma_{a,max}/\sigma_{a,1}$.

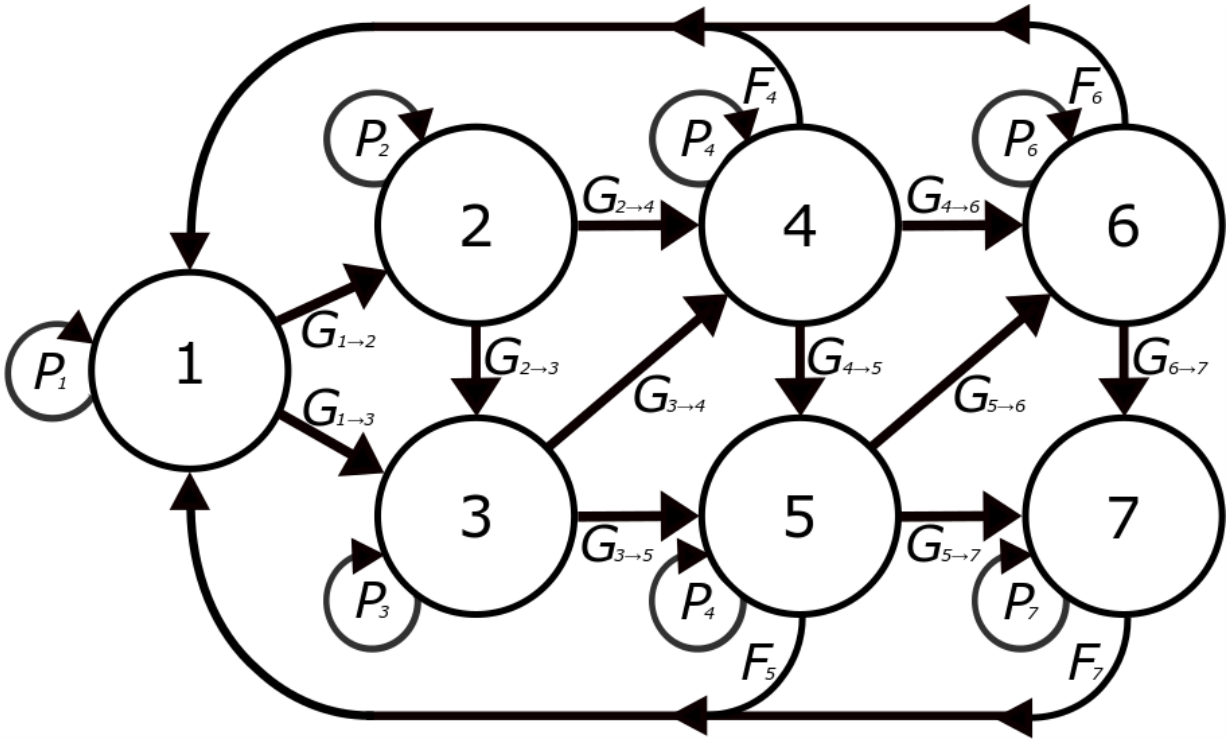

Figure 1. Generalized life cycle used to model the population dynamics of Westslope Cutthroat Trout (WCT). F_i represents stage-specific annual fertility, P_i represents the probability of surviving and remaining in stage i, and G_i represents the probability of surviving and moving to stage i+1 or i+2 each year.

THE MODEL

WCT life cycle was modeled using a female only, density-dependent, birth-pulse, pre-breeding, length-based, stage-structured population matrix model with annual projection intervals (Caswell 2001; Figure 1). Stages were defined based on length because many life-history characteristics of WCT correlate better with length than age, such as maturity (Downs et al. 1997).

The matrix consisted of 7 stages (Figure 1) defined by WCT growth (see above). The divisions between stages were determined by taking the mid-point between mean size-at-age; between successive age classes pre-maturity (stages 1–4) and between every second age post maturity (stages 5 and 6) with all individuals > 203 mm categorized into stage 7 (Table 1).

The projection matrix **A** is the product of the transition matrix **B**, consisting of the life history characteristics, and the density-dependence matrix **D** (see Equation 16 below) representing the density-dependence effects, where:

$$\mathbf{B} = \begin{bmatrix} P_1 & 0 & 0 & F_4 & F_5 & F_6 & F_7 \\ G_{1\to2} & P_2 & 0 & 0 & 0 & 0 & 0 \\ G_{1\to3} & G_{2\to3} & P_3 & 0 & 0 & 0 & 0 \\ 0 & G_{2\to4} & G_{3\to4} & P_4 & 0 & 0 & 0 \\ 0 & 0 & G_{3\to5} & G_{4\to5} & P_5 & 0 & 0 \\ 0 & 0 & 0 & G_{4\to6} & G_{5\to6} & P_6 & 0 \\ 0 & 0 & 0 & 0 & G_{5\to7} & G_{6\to7} & P_7 \end{bmatrix} \quad (8)$$

and:

$$\mathbf{A} = \mathbf{B} \circ \mathbf{D}, \quad (9)$$

where the symbol ∘ represents the Hadamard product or the element by element multiplication of the matrices.

Table 1. Stage definitions based on length and mean length of individuals in stage i.

Stage	Length range (mm)	Mean length (mm)
1	< 52	33.5
2	52 – 86	70.1
3	86 – 114	101.0
4	114 – 138	127.1
5	138 – 175	156.2
6	175 – 203	188.7
7	> 203	217.5

Stage-based matrix models incorporate estimates of F_i, stage-specific fertility; P_i, the probability of survival and remaining in stage *i*, and G_i, the probability of surviving and moving to the next stage. As a length-based model it is possible that individuals with rapid growth skip a stage; to accommodate growth variation, the matrix included 2 stage-specific estimates of G, $G_{i\to i+1}$ and $G_{i\to i+2}$.

Fertility, F_i, is the product of all reproductive parameters and as a pre-breeding matrix also incorporates the probability of surviving from the egg stage to age-1 ($\sigma_e\sigma_0$):

$$F_i = f_i\varphi\theta_i\pi_i\sigma_e\sigma_0 T\ . \quad (10)$$

P_i and G_i each are a function of stage-specific survival (σ_i) and stage-specific transition probabilities (τ_{i+1} and τ_{i+2}) describing the likelihood of moving from stage i to $i+1$ and from stage i to $i+2$ respectively, where:

$$P_i = \sigma_i\big(1 - (\tau_{i+1} + \tau_{i+2})\big), \quad (11)$$

$$G_{i\to i+1} = \sigma_i\tau_{i+1}, \text{ and} \quad (12)$$

$$G_{i\to i+2} = \sigma_i\tau_{i+2}. \quad (13)$$

Stage-specific transition probabilities were estimated from growth simulations. Mean growth increments were calculated from the VBGF (Equation 1) and stochastically varied assuming annual growth increments follow a normal distribution with a standard deviation of 6.25 (Carim et al. 2017). From the resulting distribution the probability of moving between stages was determined (Table 2).

Table 2. Stage-specific parameter values used to calculate matrix values, P_i, G_{i+1}, G_{i+2}, and F_i for populations with λ = 1. σ_i represents stage-specific survival rates, τ_i represents the transition probability between stages, f_i represents fecundity, θ_i represents the proportion of females mature in each stage, and π_i represents the relative effect of maternal size on egg survival.

Stage	σ_i	τ_{i+1}	τ_{i+2}	f_i	θ_i	π_i
1	0.30	0.97	0.02	0	0	NA
2	0.40	0.90	0.07	0	0	NA
3	0.50	0.82	0.11	0	0	NA
4	0.55	0.89	0.00	166.4	0.06	0.65
5	0.60	0.49	0.02	201.0	0.99	0.76
6	0.60	0.49	NA	239.7	1.00	0.89
7	0.60	NA	NA	274.0	1.00	1

Stochasticity

Stage-specific fecundity and survival were varied annually to simulate environmental stochasticity in vital rates. The amount of variability incorporated into vital rates was set to allow fluctuations in population size to vary with a coefficient of variations (CV) of 0.15. Fecundity was assumed to follow a lognormal distribution with means estimated from Equation 3 and a standard deviation of 4 (on the normal scale). A high degree of intra-annual correlation among life-stages was assumed in stochastic fecundity and the correlation coefficient was set to 0.9 such that residuals in egg production were similar across ages classes within a year.

Survival rate was varied as instantaneous mortality ($\sigma_i = e^{-M_i}$). *M* was assumed to vary following a normal distribution with a CV of 0.165. Stochasticity for *M* was executed using the stretched-beta distribution (i.e., the normal distribution was converted to a stretched-beta distribution) to remove the extreme tails of the normal distribution and prevent *M* from being negative but maintain the mean and standard deviation (Morris and Doak 2002). *M* was assumed to correlate intra-annually among size classes with an AR1 correlation structure (correlation diminishes as distance between stages increases) and a correlation coefficient of 0.75. Egg and YOY survival were assumed to vary independently of each other and the following stages (correlation = 0).

Density-dependence

Density-dependence was assumed to act on all life-stages (*s*): eggs, YOY, juveniles, and adults. Density-dependence in each life stage acted independently and was structured as a Beverton-Holt relationship where egg density-dependence (d_e) was defined as:

$$d_e = \frac{{\sigma_{e,max}}/{\sigma_{e,1}}}{1+{b_e}/{K_e \times N_e}}, \quad (14)$$

and density-dependence of the other life-stages (d_s) was defined as:

$$d_s = \frac{\sigma_{a.max}/\sigma_{a,1}}{1+{b_a}/{K_s \times N_s}}. \quad (15)$$

Where N_s represents the current stage density, K_s is the carrying capacity for each life stage (the density that results in λ = 1), and b_a and b_e are the density-dependent coefficients (Table 3). The density-dependent coefficient values were solved for by setting Equations 14 and 15 to carrying capacity (i.e., d_e and d_s = 1).

Carrying capacity was defined at the adult stage and then estimated for all other life-stages using the stable-stage distribution (i.e., if the carrying capacity of the adult stage (K_a) was set to 500 the carrying capacity for the juvenile stage (K_j) was set as the amount of juveniles necessary to result in 500 adults, 1,657).

Table 3. Density-dependence parameters.

Symbol	Definition	Value
$\sigma_{a.max}$	*Maximum mean adult survival rate*	*0.85*
$\sigma_{a,1}$	*Mean adult survival rate at λ = 1*	*0.60*
$\sigma_{e,max}$	*Maximum egg survival rate*	*1.00*
$\sigma_{e,1}$	*Mean egg survival rate at λ = 1*	*0.65*
b_a	*Density-dependence parameter*	*0.417*
b_e	*Density-dependence parameter for egg survival*	*0.538*

The density-dependence matrix, **D**, was structured as:

$$\mathbf{D} = \begin{bmatrix} d_j & 1 & 1 & d_e d_0 & d_e d_0 & d_e d_0 & d_e d_0 \\ d_j & d_j & 1 & 1 & 1 & 1 & 1 \\ d_j & d_j & d_j & 1 & 1 & 1 & 1 \\ 1 & d_j & d_j & d_j & 1 & 1 & 1 \\ 1 & 1 & d_j & d_j & d_a & 1 & 1 \\ 1 & 1 & 1 & d_j & d_a & d_a & 1 \\ 1 & 1 & 1 & 1 & d_a & d_a & d_a \end{bmatrix}. \quad (16)$$

IMPACT OF HARM

The impact of anthropogenic harm to a WCT population was assessed with deterministic elasticity analyses of the matrix and stochastic simulations.

Elasticity analysis of matrix elements provides a method to quantify the impact of changes to vital rates on a population. Specifically, elasticities measure the proportional change to population growth rate (λ) or equilibrium density (N) that results from a proportional change in a vital rate (v). For example, an elasticity of λ value of 0.2 for juvenile survival indicates that a 10% change in juvenile survival rate (e.g., $0.5 \times (1 + 0.1) = 0.55$) would cause a 2% increase in population growth rate (e.g., $1 \times (1 + 0.1 \times 0.2) = 1.02$). The elasticity of N functions the same way except acting on stage-specific densities; for example, an elasticity of N value for adult density of 0.15 for perturbations to juvenile carrying capacity (K_j) would indicate that a 15% decrease in K_j (e.g., $1{,}657 \times (1 - 0.15) = 1{,}408$) would cause a 2.25% decrease in adult equilibrium density (e.g., $500 \times (1 - 0.15 \times 0.15) = 489$).

Elasticities are useful as they allow for assessment of how impactful changes to vital rates and other model parameters are to a population and because they represent proportional changes their values are directly comparable. They are preferable to simulation analyses because of the speed they can be estimated allowing for many more perturbations to be examined than simulations. Elasticities are limited, however, as they represent permanent changes and assume all other model parameters remain unchanged. Therefore, simulation analysis was used to examine the effects of transient or periodic harm to a population.

Elasticity of λ

Elasticities of λ (ε_λ) are calculated by taking the scaled partial derivatives of λ with respect to a vital rate (ν; Caswell 2001):

$$\varepsilon_\lambda = \frac{\nu}{\lambda}\sum_{i,j}\frac{\partial\lambda}{\partial a_{i,j}}\frac{\partial a_{i,j}}{\partial \nu}, \quad (17)$$

where a_{ij} is the projection matrix element in row *i* and column *j*.

Elasticity estimates are influenced by current conditions. Therefore, elasticity values are provided for 4 population states: declining, stable, growing and booming. A declining population was defined based on COSEWIC criterion A2 for Threatened species: a ≥ 30% reduction in population size over 10 years or 3 generations, whichever is longer; resulting in λ_{min} = 0.982. A stable population is defined as one with λ_1 = 1. A booming population was one with all vital rates set to maximum values, i.e., when density is 0; resulting in λ_{max} = 1.52. Finally, a growing population was defined by setting vital rate values as if population size was at 50% of carrying capacity; resulting in λ_{mean} = 1.2.

Elasticity of N

Elasticities of N (ε_N) are calculated from the sensitivities of N ($\frac{d\widehat{\mathbf{N}}}{d\boldsymbol{v}^\intercal}$) where (Caswell 2019):

$$\frac{d\widehat{\mathbf{N}}}{d\boldsymbol{v}^\intercal} = \left(\mathbf{I}_i - \mathbf{A} - \left(\widehat{\mathbf{N}}^\intercal \otimes \mathbf{I}_i\right)\frac{\partial vec\mathbf{A}}{\partial \mathbf{N}^\intercal}\right)^{-1}\left(\widehat{\mathbf{N}}^\intercal \otimes \mathbf{I}_i\right)\frac{\partial vec\mathbf{A}}{\partial \boldsymbol{v}^\intercal}, \quad (18)$$

and:

$$\varepsilon_{\mathrm{N}} = diag\left(\widehat{\mathbf{N}}\right)^{-1}\frac{dN}{d\boldsymbol{v}^\intercal}diag(\boldsymbol{v}). \quad (19)$$

$\mathbf{A}$ is the projection matrix of dimension $i \times i$, $\mathbf{I}_i$ is an identity matrix of dimension $i \times i$, $\widehat{\mathbf{N}}$ is a vector of equilibrium densities, $\frac{\partial vec\mathbf{A}}{\partial \mathbf{N}^\intercal}$ is the partial derivatives of matrix $\mathbf{A}$ with respect to stage densities, $\frac{\partial vec\mathbf{A}}{\partial \boldsymbol{v}^\intercal}$ partial derivatives of matrix $\mathbf{A}$ with respect to the vital rates or model parameters of interest, $^\intercal$ is the transpose operator and $\otimes$ represents the Kronecker product. $diag\left(\widehat{\mathbf{N}}\right)$ and $diag(\boldsymbol{v})$ represent diagonal matrices with the equilibrium densities and parameter values on the diagonal respectively and 0s on the off diagonal entries. See Caswell (2019) for more details.

The initial parameterization of the model assumes that habitat (or whatever resource determines K_s) is limiting at all stages (i.e., there is only enough resources at each stage to allow for the pre-determined adult density). This is likely not the case in many systems. Therefore, estimates of elasticities of N were made under conditions where all habitat types are limited as well as when there is surplus habitat at each life-stage. This was accomplished by increasing carrying capacity of that life-stage 10-fold while keeping the other stages' carrying capacity constant.

Simulation

Simulation analysis was used to investigate the impacts of periodic stage-specific harm on adult population density. Stage-specific survival rates were reduced by some level of harm, ranging from 0 to 99%, at different frequencies: 1, 2, 5, and 10 years, over a 100 year simulation. The initial carrying capacity was then compared to the mean population size over the final 15 years of simulation to determine the effect of the harm, quantified as the proportion of initial K_a. The frequency indicates how often harm was applied. A frequency of 1 indicates that harm is constant and applied every year, where a frequency of 10 indicates that harm is periodic and applied once every 10 years. As a density-dependent model, it is assumed that the population is

able to recover in between applications of harm as conditions are returned to the initial state and no competitors exist as this is a single-species model.

RECOVERY TARGETS

Abundance: Minimum Viable Population (MVP)

The concept of demographic sustainability was used to identify potential minimum recovery targets for WCT. Demographic sustainability is related to the concept of a minimum viable population (MVP; Shaffer 1981), and was defined as the minimum adult population size that results in a desired probability of persistence over 100 years (~ 15 WCT generations, where generation time was estimated from the projection matrix [Caswell 2001] with $\lambda = 1$ as 6.56 years), where 'adult' correspond to stages 5, 6 and 7 from the matrix model (Equation 1; Figure 1; > 138 mm). MVP was estimated using simulation analysis which incorporated environmental stochasticity and density-dependence.

Important elements incorporated in population viability analysis include: the choice of time frame over which persistence is determined, the severity and frequency of catastrophic events, and the quasi-extinction threshold below which a population is deemed unviable. The choice of time frame is arbitrary and without biological rational; however, 100 years (~ 15 WCT generations) is likely reasonable for making management decisions.

The rate and severity of catastrophic events within WCT populations is unknown. Based on a meta-analysis, Reed et al. (2003) determined that among vertebrate populations, catastrophic die-offs that resulted in a one-year decrease in population size > 50% occurred at a rate of 14%/generation on average. This result was used as a basis within MVP simulations and 3 levels of catastrophe rate were applied to allow for uncertainty: 5%/generation, 10%/generation and 15%/generation. These rates correspond to an average catastrophe frequency of 1 catastrophe every 131, 66 and 44 years respectively. The impact of a catastrophe affects all life-stages simultaneously and was drawn randomly from a beta distribution scaled between 0.5 and 1 with shape parameters of 0.762 and 1.5 (Reed et al. 2003; Figure 2), representing the probability of a 50 to 100% decline in population size. Catastrophes represent any temporary and reversible large-scale disturbance to the population, such as drought, wildfires, or freezing and may be from natural or anthropogenic causes.

Quasi-extinction represents the compounding effects of Allee effects, demographic stochasticity and inbreeding depression (Lande 1988) leading a population to extinction once the threshold is crossed. The value of the quasi-extinction threshold cannot be empirically measured; therefore, 25 adult females was used as a reasonable approximation (Morris and Doak 2002).

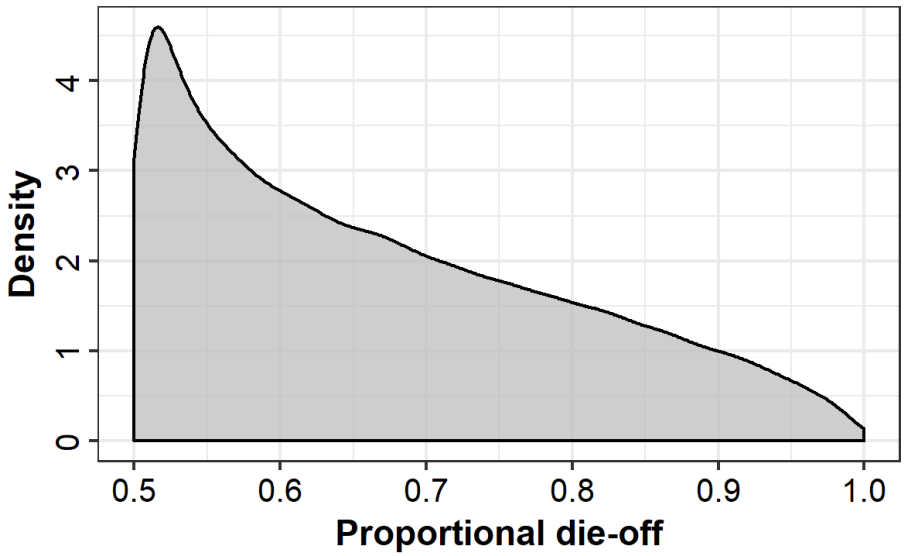

Figure 2. Beta distribution (scaled between 0.5 and 1) used in stochastic draws of catastrophe impacts. This represents the proportional decrease in population size following a catastrophic event. Shape parameters were 0.762 and 1.5 (Reed et al. 2003).

Density-dependent, stochastic simulations were conducted for populations of various initial densities (initial density represented carrying capacity, *K*, where λ = 1). Simulations were run for 100 years. Independent simulations incorporated three rates of catastrophes (0.05, 0.1 and 0.15/generation). Each simulation was replicated 5,000 times and the number of quasi-extinctions were counted. The probability of extinction (*P[ext.]*) was modelled as a logistic regression, such that:

$$P[ext.] = \frac{1}{1+e^{-(b_{MVP} log_{10}(Na)+a_{MVP})}}, \quad (20)$$

where a_{MVP} and b_{MVP} represent the fitted intercept and slope from the logistic regression. Equation 20 can be rearranged to estimate the adult population size required to give a desired level of population persistence (MVP):

$$MVP = 10^{-\frac{\log\left(1/P[ext.]-1\right)+a_{MVP}}{b_{MVP}}}. \quad (21)$$

MVP estimates are presented for quasi-extinction probabilities of 5% and 1%.

Habitat: Minimum Area for Population Viability (MAPV)

Minimum area for population viability (MAPV) is defined as the quantity of habitat required to support a population of MVP size (Velez-Espino et al. 2010).

Young et al. (2005) assessed the relationship between CRCT and Greenback Cutthroat Trout (GCT; *O. c. stomias*) population size (> 75 mm) and stream length in Wyoming and Colorado. The relationship was based on electro-fishing estimates of abundance and occupied stream length which gave a non-linear relationship: $N_{>75mm} = (0.00508 stream\ length + 5.148)^2$. This suggests that CT density increases with available habitat. COSEWIC (2016) listed abundance estimates for adult (> 153 mm) WCT in Alberta and estimates of the length of habitat occupied by each population of WCT. Data for Alberta suggests WCT density also increases with available habitat. These data were used to fit a relationship between habitat length and population size using a negative binomial regression (to account for over-dispersion) with a

square root link function (superior fit to the log link ΔAIC > 10) yielding (Figure 3; n = 38, θ = 0.96, se = 0.201, p < 0.0001):

$$N_{>153mm} = (7.55 + 0.0023 stream\ length)^2. \quad (22)$$

This relationship was used to find the expected stream length required to support MVP sized WCT populations.

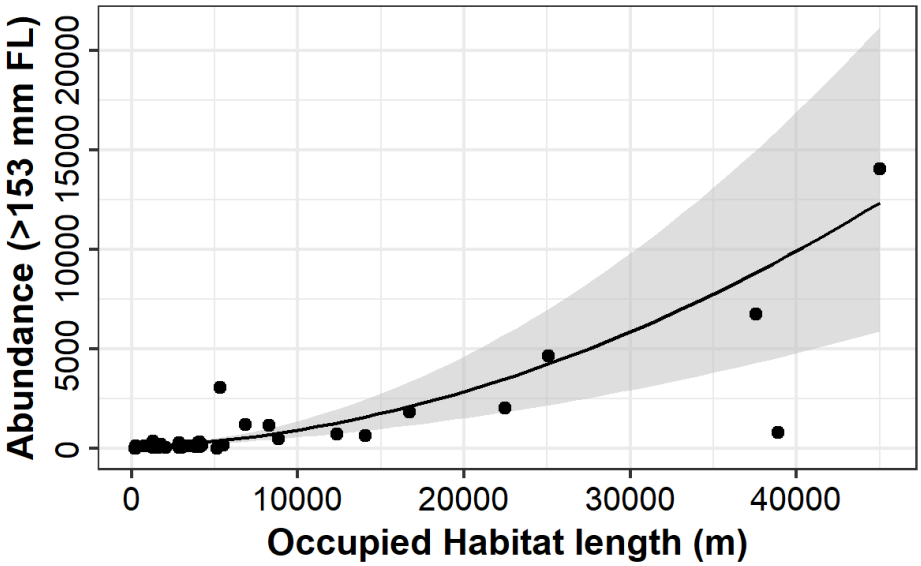

Figure 3. The relationship between occupied stream length and WCT (> 153 mm) from Alberta populations (data from COSEWIC 2016).

RECOVERY TIMES

Time to recovery was estimated using simulation analysis similar to MVP simulations. Simulations began with initial population sizes set to 10% of MVP. Simulations incorporated: stochasticity, density-dependence, and catastrophes in the same manner as MVP simulations. The population was deemed recovered when MVP was reached (MVP was also used a carrying capacity). Simulations were repeated 5,000 times. Setting carrying capacity at MVP can be viewed as the minimum habitat restoration necessary for population persistence. This assumption would result in the longest times for recovery for a viable population. If carrying capacity were greater than MVP, recovery times would be shortened.

RESULTS

IMPACT OF HARM

Three analyses were used to assess the impact of harm to WCT populations (Table 4): deterministic elasticity analysis on population growth rate (Figure 4) and life-stage density (Figure 5), and stochastic simulation analysis (Figure 6).

Table 4. Comparison of a subset of elasticity results from three analyses. Elasticity of λ values represent the proportional change in λ that results from a proportional change in a vital rate assuming a growing (λ_{mean} = 1.2) population. Elasticity of N values represent the change in adult density that results from a proportional change in a vital rate. Simulation results represent the proportional change in adult density that result from an annual proportional change in vital rate (estimated from 10% harm values).

Parameter	Elasticity of λ	Elasticity of N	Simulation
f	0.16	0.01	NA
σ_0/σ_E	0.16	0.02	0.06
σ_j	0.58	2.30	2.22
σ_a	0.26	1.05	1.03
K_e	NA	0.01	NA
K_0	NA	0.01	NA
K_j	NA	0.68	NA
K_a	NA	0.31	NA

Elasticity of λ

The elasticity to λ to perturbations of vital rates (Figure 4) gives an indication of how the population may respond to changes in vital rates; positive values indicate that population growth rate will increase if the vital rate is increased. Elasticity estimates are presented for fertility (F) which encompasses all parameters contributing to Equation 10 including egg and YOY survival rates, transition probabilities (τ) and survival rates (σ) for the juvenile and adult stage.

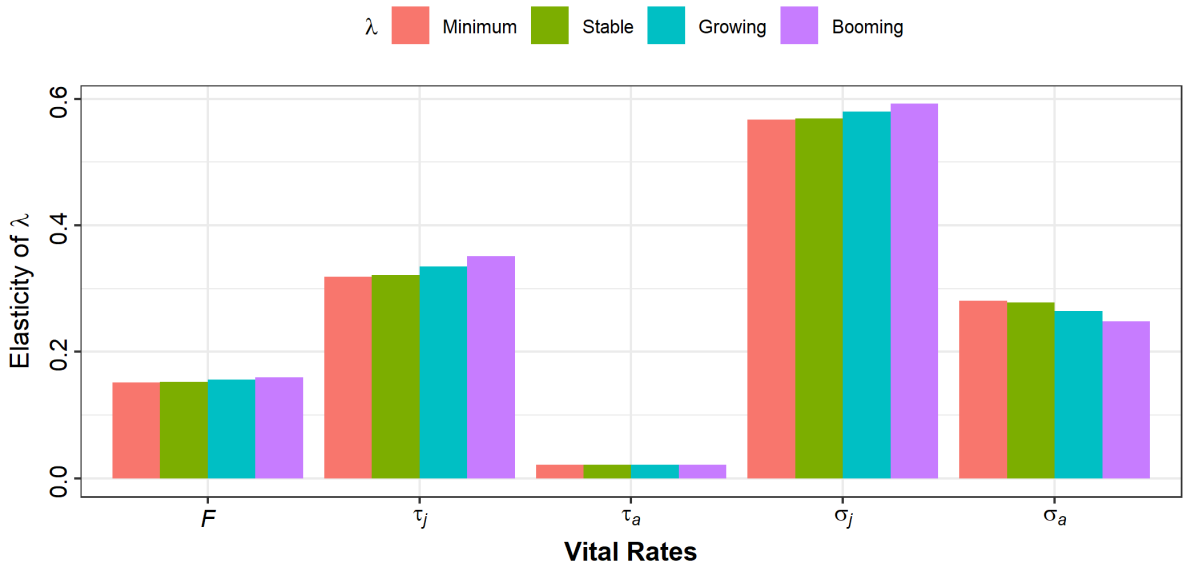

Figure 4. Elasticity of λ analysis results under 4 population states: declining, stable, growing and booming. F represents fertility and represents independent perturbations to any parameters that contributes to fertility (Equation 10), τ represents the transition probability, and σ represents survival for the juvenile (j) and adult (a) stages.

The results were similar across different rates of population growth. Population growth rate was most sensitive to changes to juvenile survival with elasticity values ~ 0.57. This was greater than the sensitivity of λ to adult survival (~ 0.27) or YOY/egg survival (~ 0.15). This indicates that a population of WCT would be most affected by mortality at the juvenile stage (assuming density-independence). For example, a mortality rate of 5% on top of natural mortality would cause a stable population (λ = 1) to experience an almost 3% decline in population size

annually ($1 \times (1 - 0.05 \times 0.57)$). After juvenile survival, λ was most sensitive to the transition rates within the juvenile stage (i.e., stages 1-4) with values ~ 0.32; indicating that increases in somatic growth rate will correspond to increases in population growth rate.

Elasticity of N

The above analysis of elasticities of λ assumes density-independence but if density-dependence acts on the populations the results may not hold. Therefore analysis of the elasticity of life-stage-specific density (N_s) to vital rates was applied to investigate how population size may change with density-dependence acting across different life-stages. The initial model conditions have density-dependence acting on all life stages with population size limited (perhaps by habitat) at each stage. If carrying capacity is assumed to be limited by habitat (K_s may be limited for other reasons, however, habitat is perhaps the easiest to visualize) at each life-stage independently, the way that elasticity of N values change when surplus habitat is available for each life-stage can be determined. The effect of changes to fecundity, survival rates and stage-specific carrying capacity (K_s) have on stable juvenile, adult, and whole population densities were investigated (Figure 5).

Similar to the elasticity of λ analysis, typically, changes to juvenile survival rate (combined matrix stages 1:4) had the greatest effect on adult population size. Changes to fecundity and egg/YOY survival rate only affected the number of juveniles in the population but because of density-dependence acting during the juvenile stage there was often a negligible and sometime negative effect on adult population size. A negative elasticity indicates that increases in that vital rate would lead to a decrease in adult density. The exception to this was when there was surplus juvenile habitat (Figure 5, panel 4 – surplus juvenile habitat). Under these conditions, with little or no density-dependence acting at the juvenile stage, mortality to eggs or YOY WCT were as influential on adult density as mortality to adults. The elasticity values for fecundity were smaller than those of egg/YOY survival which differs from the results of the elasticity of λ where they were equal (Figure 4). Changes to adult survival typically did not increase the adult population size as much as increasing juvenile survival unless there was surplus adult habitat available (Figure 5, panel 5 – surplus adult habitat).

The elasticity values for juvenile survival on adult density were 2.3 when all habitat types were limiting and 3.1 when surplus juvenile habitat was available. The elasticity values for adult survival rate were 1.1 when all habitat types were limiting and 2.8 when surplus adult habitat was available. These values can be used to determine the change in adult density expected from changes in vital rates. For example, if a population with an initial abundance of 500 adults experienced an additional mortality of 10% (e.g., fishing mortality) to the juvenile stage the adult population would decrease by 115 adults ($500 \times 2.3 \times 0.1$) if habitat is limited at all stages and 155 ($500 \times 3.1 \times 0.1$) if there was surplus juvenile habitat. If instead the mortality acted on the adult stage there would be decreases of 55 ($500 \times 1.1 \times 0.1$) and 140 ($500 \times 2.8 \times 0.1$) when all habitat types are limiting or surplus adult habitat was available respectively.

Results for changes in stage-specific carrying capacity are also presented (Figure 5). Similar to changes in survival rates with all habitat types limiting the greatest effect on adult population size results from changes to juvenile carrying capacity (ε_N = 0.68). Changes to adult carrying capacity were next most influential (ε_N = 0.31) and the effects of changes to spawning or YOY habitat were negligible. When surplus habitat is available for a life-stage then changes to carrying capacity for that life-stage had a negligible effect on population size. For example, when surplus juvenile habitat is available (Figure 5, panel 4 – surplus juvenile habitat) changes to juvenile carrying capacity did not increase adult density, instead changes to adult carrying capacity had the great impact on density. As well, under these conditions, there was an effect of changes to spawning and YOY habitat on adult density (ε_N = 0.22 and 0.26).

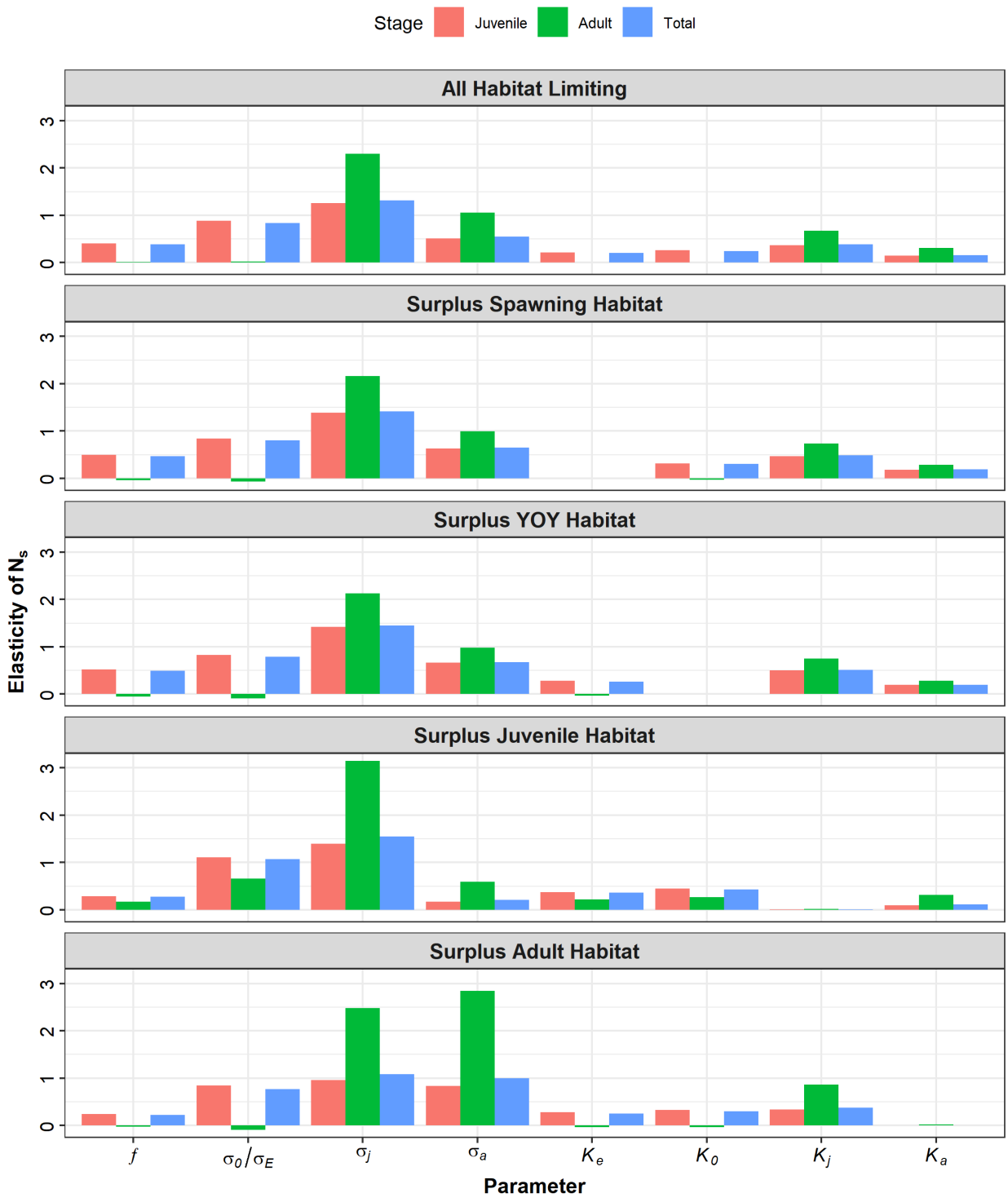

Figure 5. Elasticity of N_s analysis results for populations with different limitations on density. In the top panel all habitat types are limiting and in the bottom 4 panels one habitat type is in surplus. f represents total fecundity, and σ_s represents life-stage-specific survival and K_s represents life-stage-specific carrying capacity.

Simulation

The above elasticity analyses assume that any change to a vital rate is permanent. Simulation analysis was used to investigate how the population may respond to periodic perturbations occurring annually (for comparison to elasticity analysis), every second year, fifth year, and tenth year (Figure 6). An arbitrarily chosen reference line was included at the point where adult density reduced to 75% of initial carrying capacity.

Similar to the elasticity analysis, harm to juvenile stage (increases in annual mortality) had the greatest impact on adult density of the stage-specific harm. The lower confidence interval for juvenile survival crossed the 75% threshold when harm equalled 0.06 indicating that that an additional mortality of 6% on juveniles could cause adult density to decrease 25% from initial pre-harm densities. The lower confidence values for adult and YOY stages were 0.13 and 0.49 respectively. The lines for YOY and adult harm cross each other at approximately 0.86 (Figure 6, top left panel) as the impact of harm to YOY fish accelerates at large values while the impact of adult harm plateaus because some stage-4 WCT are able to reproduce and are not impacted by ‘adult’ harm.

As the frequency of harm decreases the effects of harm decreases as well. With biennial harm lower confidence intervals cross the 75% threshold at approximately double the value of annual harm. At 5 year harm intervals adult population size was not greatly affected by harm to YOY WCT, while juvenile and adult harm of > 28 and 54% could cause a 25% decline in population size. At 10 year harm intervals, harm to the adult stage only resulted in small population declines while harm to juvenile was still impactful when mortalities exceed 65%. If the population as a whole is impacted, however, mortalities greater then 41% occurring every 10 years could result in the population declining to 75% of initial densities.

These simulations assume that the environment and vital rates return to initial conditions immediately following the application of harm and there are no large impediments to population recovery, such as significant competitors.

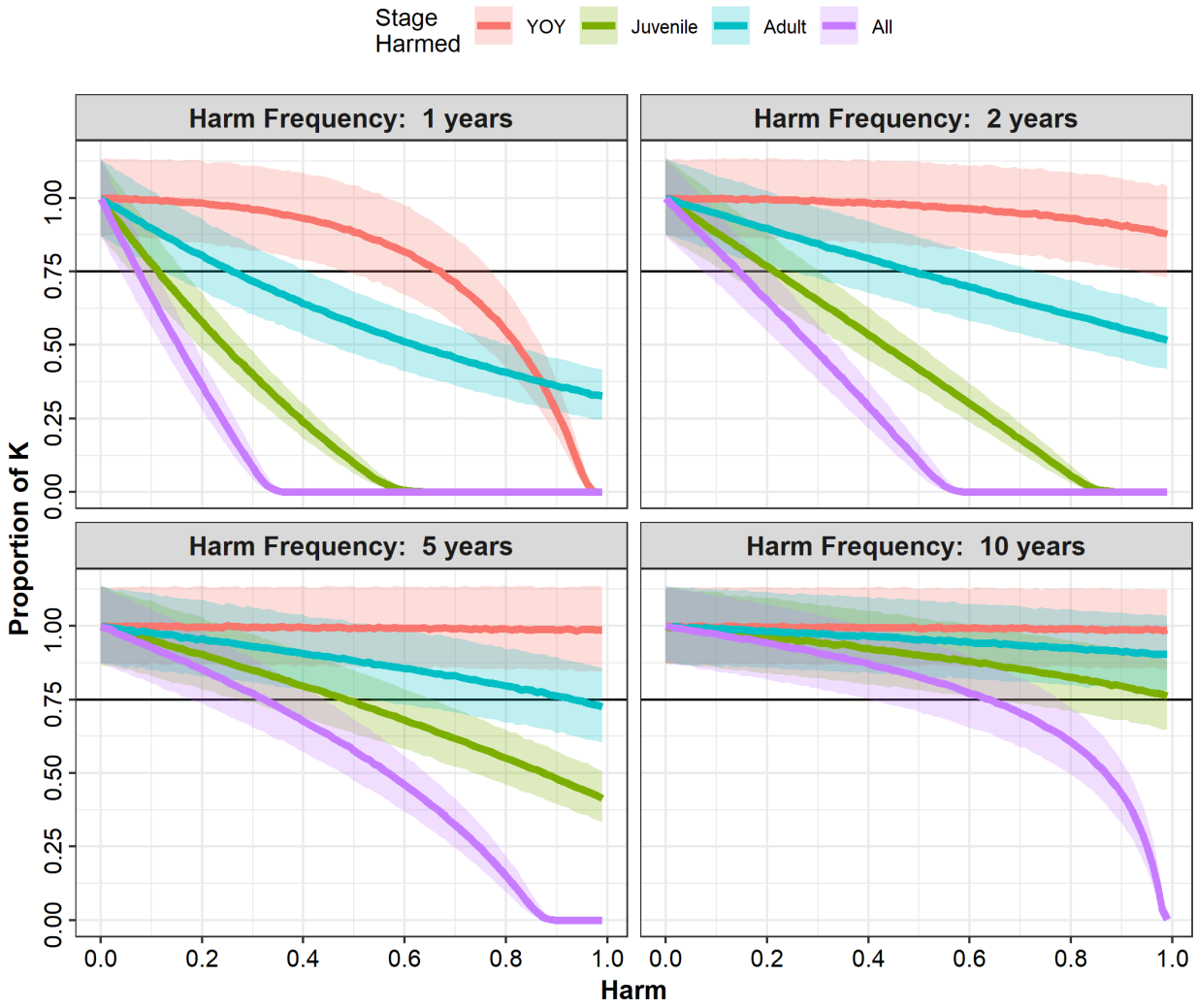

Figure 6. Results from harm simulation analysis where harm is applied at different frequencies to specific life-stages. The x-axis represent the proportional harm (e.g., annual mortality) applied to the life-stage and the y-axis represents the proportional decrease in adult density over a 100 year simulation. The solid lines represent the mean impact and the surrounding polygons represent 95% confidence intervals. The reference line indicates a 25% decline from initial density.

RECOVERY TARGETS

Abundance: Minimum Viable Population (MVP)

Demographic sustainability was assessed using stochastic, density-dependent population simulations. Simulation outputs, binomial quasi-extinctions (1: extinct; 0: extant), were fitted using a logistic regression (Figure 7).

Recovery target are presented for abundances that provide a 5% and 1% probability of quasi-extinction over 100 years (Table 5). Additional targets, those with different extinction risks, can be estimated with use of Equation 21. Simulation outputs applied solely to females in the populations. It was assumed that WCT maintain an even sex ratio throughout its life-cycle and therefore female estimates were doubled to account for males in the population (Table 5).

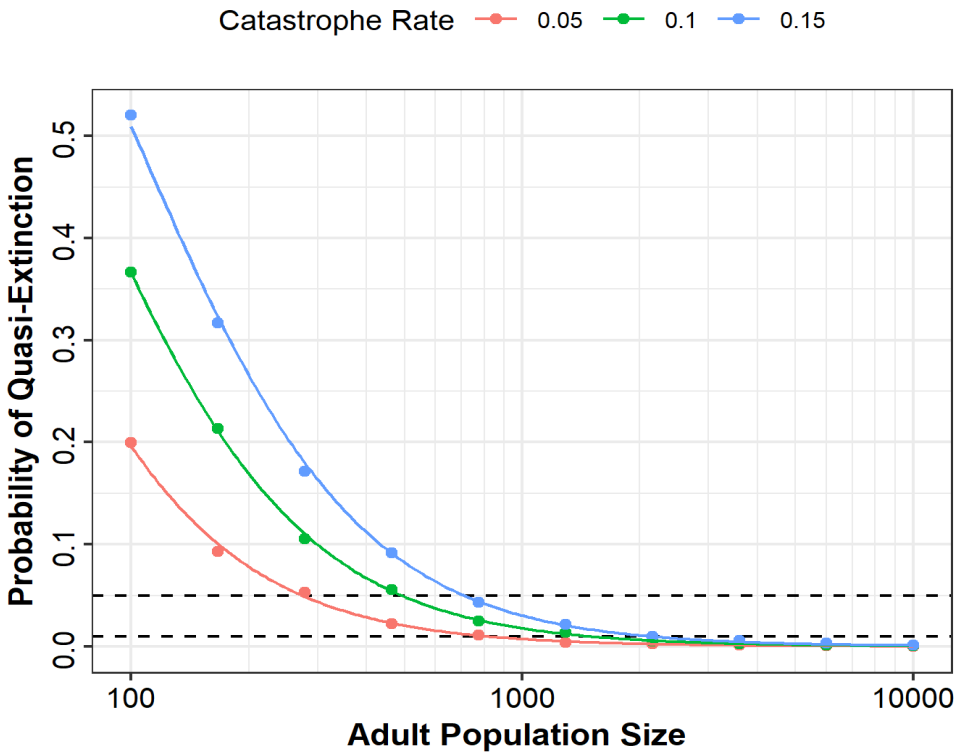

Figure 7. The probability of quasi-extinction as a function of adult female density for and three rates of catastrophe probability. The points represent mean simulation values and the lines represent fitted logistic regressions following the relationship (female abundances only): $P[ext.] = \frac{1}{1+e^{-(b_{MVP}log_{10}(N_a)+a_{MVP})}}$*, where parameters aMVP equal 5.6, 6.4, and 7.0 and bMVP equals -3.51, -3.46, and -3.50 for catastrophe rates 0.05, 0.10 and 0.15 respectively.*

Table 5. Recovery targets for adult populations size (MVP) and habitat (MAPV). MVP values represent females and males in the population assuming a 1:1 sex ratio. MAPV estimates were made by solving for the stream length predicted to give a population of MVP size (Equation 22) based on densities from Alberta populations of WCT (COSEWIC 2016). LCI represents lower confidence interval estimates and UCI represents upper confidence interval estimates.

Catastrophe Rate	MVP		MAPV (river km)					
	P[ext] = 5%	P[ext] = 1%	P[ext] = 5%			P[ext] = 1%		
			LCI	Mean	UCI	LCI	Mean	UCI
0.05	546	1,616	5.44	6.95	9.79	11.00	14.24	20.81
0.10	984	2,948	8.11	10.42	15.00	15.57	20.35	30.12
0.15	1,474	4,208	10.41	13.46	19.62	18.99	24.93	37.12

The required population size of adult WCT (matrix stage 5, 6 and 7, > 138 mm) depended on the assumed frequency of catastrophic perturbations to the populations. Relatively stable populations, with a catastrophe rate of 5% per generation required ~550 adults to achieve a 95% likelihood of persistence over 100 years and ~1,600 adults to achieve a 99% likelihood of persistence. With more frequent catastrophes, 15% per generation, adult population sizes of ~1,500 and ~4,200 of 95 and 99% persistence probabilities respectively.

Habitat: Minimum Area for Population Viability (MAPV)

Habitat quantity required to support a population of WCT was estimated by solving for the stream length predicted to give a population of MVP size (Equation 22). From this relationship the expected mean stream lengths and confidence intervals for each MVP estimate was estimated (Table 5). Depending on the level of population persistence desired and the assumed frequency of catastrophes MAPV ranged from ~7 to 24 river km based on the mean estimates of density. Using the more conservative upper confidence interval (UCI) estimates of stream length MAPV ranged from ~10 to 37 river km.

RECOVERY TIMES

Time to recovery was estimated with simulation analysis. Initial population size was set to 10% of MVP. Simulations were run to determine the time to reach MVP population size (MVP also acted as carrying capacity). These simulations reflect an increase in available habitat or a reduction in threats such that vital rates return to a pre-threat state allowing population size to increase towards carrying capacity.

Simulation replicates resulted in a distribution of recovery times (Figure 8). Recovery time was estimated as the 95th percentile of simulations; therefore 95% of simulations experience recovery by the recovery time estimate. Across all catastrophe rates and persistence probabilities recovery times ranged from 27 to 33 years.

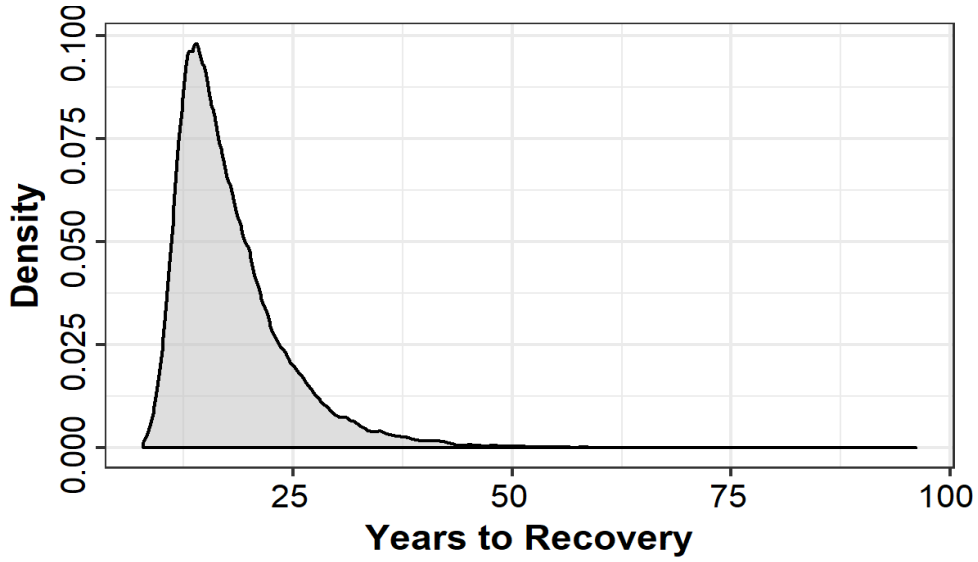

Figure 8. The distribution of recovery time-frames from all simulations for WCT populations given a recovery target of MVP and initial abundance of 10% of MVP.

DISCUSSION

A population model for WCT was created to make predictions on how a population may respond to anthropogenic harm, estimate recovery targets for abundance and habitat, and project recovery timeframes. The model represents populations of pure WCT of the stream-resident life-history type in Alberta. Other life-history types experience different rates of growth and potentially differ in other vital rates (COSEWIC 2016) and, therefore, would not be well represented by this model.

Multiple methods were used to assess the impact of harm to WCT populations. Across the various methods it becomes clear that stream-resident populations of WCT are most impacted by perturbations to the juvenile stage; however, under certain condition (e.g., surplus habitat) other life stages were equally or more important. This result holds for assumptions of density-independence and -dependence and periodic harm. Simulation analysis (Figure 6) indicated that annual mortalities of only ~6% to the juvenile stage (based on the lower confidence interval) could cause adult population size to decline 25%. Elasticity analysis of N (Figure 5) gave similar results indicating that mortalities to the juvenile stage between ~8 and 12%, in addition to natural mortality, could cause populations to decline to 75% of carrying capacity, under various habitat limitation scenarios (calculated as: $\frac{75-100}{100}/\varepsilon_{N,Sj}$). Simulation analysis showed that an additional mortality of 13% acting on the adult stage would be required to cause the same decline in density. The results from the elasticity of N analysis showed that 25% declines in N_a resulted from adult mortalities of 9%–42%. The impact of adult mortalities was greatest when there was surplus adult habitat and least when there was surplus juvenile habitat due to density-dependence effects counteracting the effects of anthropogenic harm. The effects of harm to the YOY stage were typically much lower requiring mortalities > 49% in addition to *M* to result in 25% declines in N_a based on simulation results. Although, with surplus juvenile habitat the impacts of harm to egg or YOY WCT were similar to harm to the adult stage (Figure 5).

Simulation analysis was required to investigate the impact of harm occurring periodically (at greater than 1 year intervals) as sensitivity analysis assumes all perturbations are permanent. The impact of harm decreased relatively linearly with decreased frequency, where the amount of harm that resulted in a 25% decline in N_a at different harm frequencies was approximately equal to the impact of annual harm divided by frequency. This indicates that the more recovery time allowed following periodic harm the smaller the impact of each incidence of harm.

Carim et al. (2017) estimated the elasticity of λ for populations of WCT in Montana and, similar to this analysis, found a greater impact of perturbations early in life with a decline in elasticities as body length exceeded 150 mm. Aggregated to life-stage, the results correspond well to those of this analysis demonstrating a greater importance of the juvenile stage (Carim et al. 2017). Hilderbrand (2003) applied sensitivity analysis of λ to matrix elements of a length-based CT matrix model. Their analysis differs as sensitivities represent absolute changes in parameter values rather than proportional changes and the analysis was preformed on matrix elements rather than vital rates. Nonetheless, Hilderbrand (2003) found an increased importance of sub-adults that will mature the following year and YOY fish, showing again the significance of sub-adults in CT populations.

Estimates of recovery targets were provided for abundance using simulation analysis to determine population sizes required for demographic stability through estimates of MVP. Depending on the assumed rate of catastrophic die-offs (5 to 15% per generation of a ≥ 50% population decline), an adult (> 138 mm) population size of 550–1,500 and 1,600–4,200 was required to achieve a 95% or 99% likelihood of persistence over 100 years respectively. The frequency of catastrophes is an unknown variable and was very impactful on model results. Ultimately, it represents how stable the environment is expected to be over long timeframes. The rate of catastrophe may vary among locations and therefore the most appropriate recovery target will also vary. Estimates based on more frequent catastrophes are more conservative especially if the frequency of large scale stochastic disturbances increases with climate change (Williams et al. 2009).

Reed et al. (2003) conducted a meta-analysis to determine the frequency of large (> 50%) inter-annual changes in abundance for vertebrate species. Across all species there was an observed population disturbance occurring at a rate of 14%/generation (Reed et al. 2003). This result was

used to guide what rates were included in simulation models. Although species-specific research that identifies the magnitude and frequency of catastrophic events at the population level would greatly reduce uncertainty in estimates of MVP size.

Previous analyses have estimated MVP for WCT with abundances smaller and greater than estimates from this analysis. Hilderbrand (2003) used a simulation model to estimate extinction risk of populations with different carrying capacities and found that populations with abundances (age-1+) > 2,000 had a < 5% extinction risk over 100 years. These results did not explicitly incorporate stochastic catastrophes but did include environmentally stochasticity where survival and transition probability were varied as a normal distribution with a standard deviation (SD) of 0.09. Simulations which included immigration (exchange between two uncorrelated populations) vastly reduced the risk of extinction with extinction risk decreasing further as immigration rates increased. The effect of immigration diminished as the correlation in environmental stochasticity between the two populations increased (Hilderbrand 2003). Mayhood (2014) used empirical relationships to predict persistence over 40 generations (author stated this is approximately 120–200 years) where: $P[persistence] = 18.375 \ln(N) - 64.866$. This relationship predicts population sizes of ~6,000 and ~7,500 to achieve persistence probabilities of 5% and 1% respectively. The greater timeframe likely magnified Mayhood's (2014) estimates relative to this analysis.

Additional analyses have examined the persistence likelihoods of extant populations of various subpopulations of CT and found that generally persistence probabilities of CT populations are low. Roberts et al. (2017) and Zeigler et al. (2019) used Bayesian network models for CRCT and Rio Grande Cutthroat Trout (RGCT; *O. c. virginalis*) to determine persistence probabilities of location-specific populations. Roberts et al. (2017) identified the greatest threat to CRCT was further invasion by non-native Brook Trout which threatened to extirpate 39% of extant populations. A further 37% of populations were threatened by extinction due to increased environmental stochasticity in short stream fragments. Persistence probabilities to the year 2080 for RGCT were generally low, ranging from 0 to 90% with only 11% of populations estimated to have a > 75% likelihood of persistence (Zeigler et al. 2019). Populations of RGCT were most threated by presence or potential invasion by non-native trout species with warming from climate change the other most significant threat (Zeigler et al. 2019).

Estimates of abundances for MVP were converted into habitat requirements through a relationship between stream length and abundance for Alberta (Figure 3). This relationship predicts densities ranging from 78 to 169 adult (> 153 mm) WCT/km based on the mean relationship and from 56 to 113 adults/km based on the Lower Confidence Interval (LCI; Figure 3). Using the more conservative upper confidence intervals MAPV (Table 5), habitat estimates range from 9.8 to 37.1 km of stream habitat. Hilderbrand and Kershner (2000) made estimates of stream lengths required to support 2,500 cutthroat trout (> 75 mm) assuming high densities of 300 fish/km and low densities of 100 fish/km and found comparable results to this analysis of 9.3 and 27.8 km of stream habitat. As well, Roberts et al. (2013) identified that stream length < 7 km increased the risk of extinction because of the associated effects on abundance and the lack of sufficient refuges from stochastic disturbances such as wildfires.

This analysis only identifies estimates of quantities of habitat that may be required by a WCT and does not address habitat quality. Young et al. (2005) found that in addition to stream length, depending on methodology, higher temperature was an important contributor to CRCT and GCT abundance as was the number of deep pools; however, the most parsimonious model included only stream length. Another important result was that bank full width of the stream did not significantly affect CT abundance; however, this may be due to inconsistencies in stream type diminishing the relationship between habitat quality for CT and stream width. Harig and Fausch (2002) used logistic regressions to predict translocation success for RGCT and GCT and found

that cold summer temperature, narrow stream width, and a lack of deep pools limited translocation success. As well, they determined that a minimum watershed area of 14.7 km^2 represented a threshold between areas with high CT abundances or those with absent or low abundance populations.

Simulation results revealed that WCT populations could reach MVP populations from initial densities of 10% of MVP within 27 to 33 years. These estimate assume MVP also acts as carrying capacity for the habitat. If carrying capacity exceeded MVP then final population size would be > MVP with MVP potentially achieved in less time.

UNCERTAINTIES

There are a number of uncertainties with the WCT model that may have had an effect on model results. Foremost, there is uncertainty with some of the parameterization of the model. For example, there were numerous reported estimates of mortality for stream-resident populations of WCT, however they varied widely, with annual survival rate values ranging from 25% (Carim et al. 2017) to 79% (Cope et al. 2016). Populations of WCT may have been subjected to fishing mortality which was not addressed in the model and therefore estimates of natural mortality incorporated into the model may have been overestimates. For this reason, the available data was used to inform the mean value incorporated in the model, however, mortality was primarily based on predictive relationships (Then et al. 2015).

Similarly, the data available to inform size-specific fecundity varied widely in literature reports. There are numerous equations to predict egg count as a linear function of fork length (Tripp et al. 1979, Downs et al. 1997, Mayhood 2012, Janowicz et al. 2018) however slope values differed significantly, ranging from 1.2 to 5.5. The relationship presented by Janowicz et al. (2018) was used as it was based on the largest sample size (n = 68), was the most contemporary, and was specific to Alberta stream-resident WCT, although, it had the shallowest slope.

The manner in which density-dependence was incorporated into the model may have an influence on results. Density-dependence was incorporated at all life-stages with each stage acting as a limiting factor on adult populations. These assumptions clearly have an influence on elasticity of N analysis (Figure 5) with results differing under different density-dependence conditions. MVP estimates were not influenced by type of density-dependence curve. What is important is that density dependence acts and the strength of the relationship. Inclusion of density-dependence allows populations to have some degree of recovery following large perturbations leading to much smaller estimates of MVP than when density-dependence is excluded (e.g., Roberts et al. 2016). The strength of density-dependence, in the model, was determined by defining an upper maximum for adult survival, 85%. This resulted in a maximum population growth rate, at 0 density, of 1.52. This upper limit was estimated from a relationship for M with von bertalanffy growth function (VBGF) coefficients and selected as M_{min} as it exceeded all field estimates of Z. It is possible that survival at low density may be greater than the estimate incorporated in to the model which would lead to a greater λ_{max}, more resilience to perturbations, and lower MVP estimates. Using a lower value for σ_{max} provide more conservative estimates of MVP.

WCT was modelled as a small isolated population, which is appropriate for many of the extant populations (COSEWIC 2016), but may not represent the ideal for recovered systems. Small populations structured as meta-populations, with migration among them, can see drastic increases in persistence probability compared to isolated populations of the same size. van der Lee et al. (2020) found a 4-fold decrease in MVP for Redside Dace (*Clinostomus elongatus*) when complex population structure was included in the model. As well, Hilderbrand (2003)

showed significant effects on persistence probability with only 2 sub-populations exchanging individuals for WCT.

Finally, as previously discussed, the frequency of catastrophic events for WCT was unknown and had significant impact on estimates of MVP. Results are presented for multiple rates of catastrophes, however, which is most appropriate is not clear. Best practices may to be use the most conservative estimates (15%/generation) as this is close to the cross taxa average for vertebrates (Reed et al. 2003) and to buffer against uncertainty.

ELEMENTS

Element 1: Estimate the current or recent life-history parameters for WCT.

The best available data were assembled to provide life-history parameters for WCT. The value for each life-history parameter used in the modelling is presented in Tables 1, 2, and 3 and throughout the Methods section.

Element 2: Propose candidate abundance and distribution target(s) for recovery

Abundance targets were estimated using population viability analysis and estimates of MVP. Simulations incorporated density-dependence, environmental stochasticity, and random catastrophes. Targets varied depending on the desired persistence probability, catastrophe rate, and maximum population growth rate (Table 5).

The extinction probability of the population, as a whole, within a DU, P_{DU}, can be calculated as a function of the number of populations, persistence of each, and correlation among them:

$$P_{DU} = \prod_{i=1}^{n} P_{pop,i}^{\frac{n}{\boldsymbol{d}^{\intercal}\boldsymbol{\rho}\boldsymbol{d}}}. \quad (23)$$

Where $P_{pop,i}$ is the population extinction probability for population *i*, *n* is the number of populations, $\boldsymbol{\rho}$ is an *n* x *n* matrix of correlation values between population (i.e., when population of geographically close and subject to similar environmental conditions), and $\boldsymbol{d}$ is a column vector of 1s of length *n*. For example, if there were three spatial distinct populations within a DU with population level extirpation probabilities of 5%, 10% and 1% the extinction probability of the population as a whole depends on the level of correlation among the populations. If the populations are entirely independent ($\rho = 0$) equation 23 reduces to the product of P_{pop} with P_{DU} = 0.005%. If, however, each population is correlated with the other at 50% ($\rho = 0.50$) the extinction risk for the species within the DU is 0.7%.

Element 3: Project expected population trajectories over a scientifically reasonable time frame (minimum 10 years), and trajectories over to the potential recovery target(s), given current WCT population dynamics parameters.

Current population abundances and trajectories are unknown for DU 1 WCT.

Element 4: Provide advice on the degree to which supply of suitable habitat meets the demands of the species both at present and when the species reaches the potential recovery target(s) identified in element 12.

The quantity of habitat required to support MVP populations of WCT was estimated through fitting a relationship between stream length and abundance (Equation 22; Figure 3). Estimates of MAPV depended on persistence probability and catastrophe rate (Figure 4). To support ~1,600 adult WCT the model predicts a mean of 14.2 km of stream habitat is required. Of the 38 habitat estimates listed in COSEWIC (2016) only 6 (16%) provide sufficient habitat. To support

~4,200 adult WCT the model predicts a UCI of 37.1 km of stream habitat is required. Of the 38 habitat estimates listed in COSEWIC (2016) only 3 (8%) provide sufficient habitat.

Element 5: Assess the probability that the potential recovery target(s) can be achieved under the current rates of population dynamics, and how that probability would vary with different mortality (especially lower) and productivity (especially higher) parameters.

Simulations were conducted for WCT populations with an initial abundance of 10% of MVP and projected time to recovery where recovery is MVP (MVP was also set as carrying capacity). WCT had a 95% chance of reaching these recovery targets after 27–33 years.

Element 6: Evaluate maximum human-induced mortality and habitat destruction that the species can sustain without jeopardizing its survival or recovery.

The impact of harm to populations of WCT was evaluated through estimates of the elasticity of λ (Figure 4), the elasticity of N (Figure 5), and simulations (Figure 6). Across each analysis, perturbations to the juvenile stage (survival, growth, and habitat) had the greatest impact to the population (Table 4).

Estimates of maximum human-induced harm can be estimated from this analysis but depend on initial condition of the population and what final state of the population is considered allowable. Maximum harm, which is defined here as an additional mortality or proportional reduction in habitat, can be estimated as:

$$Maximum\ Harm = \frac{final\ state - initial\ state}{initial\ state} \times \frac{1}{\varepsilon \times frequency}, \qquad (24)$$

Where ε, is the estimate of elasticity for the vital rate being perturbed (Table 4), frequency is the number of times per year harm is applied (i.e., 0.2 represents a 5 year periodic cycle), and state is the population parameter being measured (λ or N). For example, the elasticity of N_a for juvenile habitat (K_j) was ~ 0.7, if initial adult population size was 5,000 and one wishes to remain above 4,500 then ~ 14% of juvenile habitat could be impacted.

REFERENCES CITED

Behnke, R.J. 2002. Trout and salmon of North America. Free Press, New York, NY. 384 p.

Budy, P., Thiede, G.P., and McHugh, P. 2007. Quantification of the vital rates, abundance, and status of critical, endemic population of Bonneville Cutthroat Trout. N. Am. J. Fish. Manag. 17(2): 593–604.

Budy, P., Wood, S., and Roper, B. 2012. A study of the spawning ecology and early life history survival of Bonneville Cutthroat Trout. N. Am. J. Fish. Manag. 32(3): 436–449.

Carim, K.J., Vindenes, Y., Eby, L.A., Barfoot, C., and Vollestad, L.A. 2017. Life history, population viability, and the potential for local adaptation in isolated trout populations. Glob. Ecol. Conserv. 10: 93–102.

Caswell, H. 2001. Matrix population models: construction, analysis, and interpretation. 2nd Edition. Sinauer Associates, Sunderland, MA. 722 p.

Caswell, H. 2019. Sensitivity analysis: matrix methods in demographic and ecology. Springer Open. 299 p. https://doi.org/10.1007/978-3-030-10534-1

Cope, S., Schwarz, C.J., Prince, A. and Bisset, J. 2016. Upper Fording River Westslope Cutthroat Trout population assessment and telemetry project: Final report. Report prepared for Teck Coal Limited, Sparwood, BC. Report prepared by Westslope Fisheries Ltd., Cranbrook, BC. 266 p.

COSEWIC (Committee on the Status of Endangered Wildlife in Canada). 2016. COSEWIC assessment and status report on the Westslope Cutthroat Trout *Oncorhynchus clarkii lewisi*, Saskatchewan – Nelson River populations, Pacific populations, in Canada. Committee on the Status of Endangered Wildlife in Canada. Ottawa, ON. xvi + 83 p.

DFO. 2007a. Documenting habitat use of species at risk and quantifying habitat quality. DFO Can. Sci. Advis. Sec. Sci. Advis. Rep. 2007/038.

DFO. 2007b. Revised protocol for conducting recovery potential assessments. DFO Can. Sci. Advis. Sec. Sci. Advis. Rep. 2007/039.

Downs, C.C., White, R.G., and Shepard, B.B. 1997. Age at sexual maturity, sex ratio, fecundity, and longevity of isolated headwater populations of Westslope Cutthroat Trout. N. Am. J. Fish. Manag. 17(1): 85–92.

Duarte, C.M., and Alcaraz, M. 1989. To produce many small or few large eggs: a size-independent reproduction tactic of fish. Oecologia 80: 401–404.

Fraley, J., and Shepard, B.B. 2005. Age, growth, and movements of Westslope Cutthroat Trout, *Oncorhynchus clarki lewisi*, inhabiting the headwaters of a wilderness river. Northw. Sci. 79: 12–21.

Harig, A.L. and Fausch, K.D. 2002. Minimum habitat requirements for establishing translocated Cutthroat Trout populations. Ecol. Appl. 12(2): 535–551.

Hilberbrand, R.H. 2003. The roles of carrying capacity, immigration, and population synchrony on persistence of stream-resident Cutthroat Trout. Biol. Conserv. 110(2): 257–266.

Hilderbrand, R.H. and Kershner, J.L. 2000. Conserving inland Cutthroat Trout in small streams: how much stream is enough? N. Am. J. Fish. Manag. 20(2): 513–520.

Janowicz, M.E., Zatachowski, W., Rybczyk, A., Dalton, S., Fernandes, E., and Fontoura, N.F. 2018. Age, growth and reproductive biology of threatened Westslope Cutthroat Trout *Oncorhynchus clarkii lewisi* inhabiting small mountain streams. J. Fish. Biol. 93(5): 874–886.

Lande, R. 1988. Genetics and demography in biological conservation. Science 241(4872): 1455–1460.

Lorenzen, K. 2000. Allometry of natural mortality as a basis for assessing optimal release size in fish-stocking programmes. Can. J. Fish. Aquat. Sci. 57(12): 2374–2381.

Mayhood, D.W. 2012. Reference parameters for headwater stream populations of Westslope Cutthroat Trout in Alberta. FWR Tech. Rep. No. 2012/12-01. iii + 34 p.

Mayhood, D.W. 2014. Conceptual framework and recovery guidelines for restoring Westslope Cutthroat Trout populations in Alberta. FWR Tech. Rep. No. 2014/03-01. xii + 90 p.

Moffett, I.J.J., Allen, M., Flanagan, C., Crozier, W.W., and Kennedy, G.J.A. 2006. Fecundity, egg size and early hatchery survival for wild Atlantic Salmon, from the River Bush. Fish. Manage. Ecol. 13(2): 73–79.

Morris, W.F., and Doak, D.F. 2002. Quantitative conservation biology: theory and practice of population viability analysis. Sinauer Associates, Sunderland, MA. 480 p.

Peterson, D.P., Fausch, K.D., and White, G.C. 2004. Population ecology of invasion: effects of Brook Trout on native Cutthroat Trout. Ecol. Appl. 14(3): 754–772.

R Core Team, 2018. R: A language and environment for statistical computing. R Foundation for Statistical Computing, Vienna, Austria.

Rasmussen, J.B., Robinson, M.D., and Heath, D.D. 2010. Ecological consequences of hybridization between native Westslope Cutthroat (*Oncorhynchus clarkia lewisi*) and introduced Rainbow (*Oncorhynchus mykiss*) Trout: effects on life history and habitat use. Can. J. Fish. Aquat. Sci. 67(2): 357–370.

Reed, D.H., O'Grady, J.J., Ballou, J.D., and Frankham, R. 2003. The frequency and severity of catastrophic die-offs in vertebrates. Anim. Conserv. 6(2): 109–114.

Roberts, J.J., Fausch, K.D., Peterson, D.P., and Hooten, M.B. 2013. Fragmentation and thermal risk from climate change interact to affect persistence of native trout in the Colorado River basin. Global Change Biol. 19(5): 1383–1398.

Roberts, J.H., Angermeier, P.L., and Anderson, G.B. 2016. Population viability analysis of endangered Roanoke Logperch. J. Fish Wildl. Manag. 7(1): 46–64.

Roberts, J.J., Fausch, K.D., Hooten, M.B., and Peterson, D.P. 2017. Nonnative trout invasion combined with climate change threaten persistence of isolated Cutthroat Trout population in the southern Rocky Mountains. N. Am. J. Fish. Manag. 37(2): 314–325.

Paul, A.J., Post, J.R., and Stelfox. J.D. 2003. Can anglers influence the abundance of native and non-native salmonids in a stream from the Canadian Rocky Mountains? N. Am J. Fish. Manag. 23(1): 109–119.

Shaffer, M.L. 1981. Minimum population sizes for species conservation. BioScience 31(2): 131–134.

Then, A.Y., Hoenig, J.M., Hall, N.G., and Hewitt, D.A. 2015. Evaluating the predictive performance of empirical estimators of natural mortality rate using information on over 200 fish species. ICES J. Mar. Sci. 72(1): 82–92.

Tripp, D.B., Tsui, P.T.P., and McCart, P.J. 1979. Baseline fisheries investigations in the McLean Creek ATV and Sibbald Flat snowmobile areas, Volume I. Prepared for the government of Alberta, Department of Recreation, Parks and Wildlife, Calgary. 245 p.

van der Lee, A.S., Poesch, M.S., Drake, D.A.R, and Koops M.A. 2020. Recovery potential modelling of Redside Dace (*Clintostomus elongatus*). DFO Can. Sci. Advis. Sec. Res. Doc. 2019/034. v + 40 p.

Vélez-Espino, L.A., and Koops, M.A. 2009. Quantifying allowable harm in species at risk: application to the Laurentian Black Redhorse (*Moxostoma duquesnei*). Aquat. Conserv.: Mar. Freshwat. Ecosyst. 19(6): 676–688. doi:10.1002/aqc.1023.

Vélez-Espino, L.A., and Koops, M.A. 2012. Capacity for increase, compensatory reserve, and catastrophes as determinants of minimum viable population in freshwater fishes. Ecol. Model. 247: 319–326.

Vélez-Espino, L.A., Randall, R.G., and Koops, M.A. 2010. Quantifying habitat requirements of four freshwater species at risk in Canada: Northern Madtom, Spotted Gar, Lake Chubsucker, and Pugnose Shiner. DFO Can. Sci. Advis. Sec. Sci. Res. Doc. 2009/115.

Williams, J.E., Haak, A.L., Neville, H.M., and Colyer, W.T. 2009. Potential consequences of climate change to persistence of Cutthroat Trout populations. N. Am. J. Fish. Manag. 29(3) 533–548.

Young, M.K., Guenther-gloss, P.M., and Ficke, A.D. 2005. Predicting Cutthroat Trout (*Oncorhynchus clarkii*) abundance in high-elevation streams: revisiting a model of translocation success. Can. J. Fish. Aquat. Sci. 62: 2399–2408.

Zeigler, M.P., Rogers, K.B., Roberts, J.J., Todd, A. S., Fausch, K.D. 2019. Predicting Persistence of Rio Grand Cutthroat Trout populations in a uncertain future. N. Am. J. Fish. Manag. 39(5): 819–848.